



# Evaluation of a Tumor-Targeting, Near-Infrared Fluorescent Peptide for Early Detection and Endoscopic Resection of Polyps in a Rat Model of Colorectal Cancer

Jade E. Jones, BHS<sup>1,2</sup>, Susheel Bhanu Busi, MS<sup>3</sup>, Jonathan B. Mitchem, MD<sup>4</sup>, James M. Amos-Landgraf, PhD<sup>3</sup>, and Michael R. Lewis, PhD<sup>1,2</sup>

## Abstract

The goal of these studies was to use a tumor-targeting, near-infrared (NIR) fluorescent peptide to evaluate early detection and to guide surgical removal of polyps in a genetically engineered rat model of spontaneous colorectal cancer. This peptide, LS301, was conjugated to Cy7.5 and applied topically to the colon of adenoma-bearing Pirc rats. Ten minutes after administration, rats underwent targeted NIR laser colonoscopy. Rats were also evaluated by white light colonoscopy and narrow-band imaging, for comparison to the NIR technique. Unlike white light and narrow-band colonoscopy, NIR imaging detected unexpected flat lesions in young Pirc rats. NIR imaging was also used to assess resection margins after electrocauterization of polyps. Tumor margins remained negative at 5 weeks postsurgery, demonstrating successful polypectomy. The present studies show that NIR-targeted colonoscopy is an attractive strategy to improve screening for and resection of colorectal neoplasia.

## Keywords

colorectal cancer, colonoscopy, near-infrared fluorescence imaging, fluorescence-guided surgery

## Introduction

Colorectal cancer (CRC) is the third most commonly diagnosed and third most deadly cancer in the United States, with a projected 135 430 new cases and 50 260 deaths in 2017.<sup>1</sup> When found early and adequately removed, long-term survival approaches 100%; however, survival of those diagnosed with metastatic disease drops to only 14% at 5 years. Screening programs employing colonoscopy have consistently been shown to decrease death rates from CRC. Despite the demonstrated benefits, there is significant room for improvement, as the miss rate for lesions is reported to be >20%.<sup>2</sup> Lesion characteristics associated with difficult detection are size and flat or sessile morphology.<sup>3</sup> In the case of these tumors, removal is difficult and flat lesions have been shown to have advanced features at smaller size, making detection all the more important.<sup>4</sup> Additionally, it has been shown that 6% to 9% of screened patients have advanced lesions: large or flat tumors and those harboring preinvasive or invasive cancers.<sup>5</sup> At an early stage, these tumors can often be completely removed endoscopically for cure, allowing patients to avoid segmental

colectomy. The most important factor in the prevention of recurrence or progression is a negative margin status, that is, ensuring complete tumor removal.<sup>6</sup>

Recent advances to address the unmet need in endoscopic imaging have the potential for more sensitive detection of flat and sessile lesions than conventional white light colonoscopy. Narrow-band imaging (NBI), which utilizes the absorption

<sup>1</sup> Department of Veterinary Medicine and Surgery, University of Missouri, Columbia, MO, USA

<sup>2</sup> Research Service, Harry S. Truman Memorial Veterans' Hospital, Columbia, MO, USA

<sup>3</sup> Department of Veterinary Pathobiology, University of Missouri, Columbia, MO, USA

<sup>4</sup> Department of Surgery, University of Missouri, Columbia, MO, USA

Submitted: 19/02/2018. Revised: 06/06/2018. Accepted: 15/06/2018.

## Corresponding Author:

Michael R. Lewis, Department of Veterinary Medicine and Surgery, College of Veterinary Medicine, University of Missouri, 900 E. Campus Drive, Columbia, MO 65211, USA.

Email: lewismic@missouri.edu



maximum of hemoglobin to produce vascular contrast, was shown to have no advantage in miss rate compared to white light.<sup>7</sup> Newer imaging modalities such as chromoendoscopy, autofluorescence, and confocal laser endoscopy have been developed in attempts to improve the sensitivity of lesion detection.<sup>8</sup> However, studies have found little to no benefit of these advancements over white light colonoscopy, due to limited tissue penetrance and failure to distinguish smaller polyps and cancerous lesions from surrounding normal tissue.<sup>9,10</sup> Thus, there is a need for a targeted agent that can detect colorectal tumors in contrast with adjacent healthy tissue with high sensitivity and specificity.

Achilefu and coworkers have developed a tumor targeting, near-infrared (NIR) fluorescent peptide probe (LS301, sequence cypate-cyclo(cGRDSPC)K) for fluorescence-guided surgery in mouse xenograft models of breast cancer and liver metastasis.<sup>11,12</sup> This peptide targets unspecified integrin receptors present at tumor margins.<sup>13</sup> In 2014, their group reported the use of a miniaturized confocal laser endoscopy system and the NIR peptide probe to evaluate colonoscopy in a chemically induced mouse model of CRC.<sup>14</sup> After LS301 had accumulated in tumors, fluorescent colonoscopy showed a 6-fold increase in fluorescence between adenomas and normal tissue and a 3-fold increase between flat lesions and normal tissue. These results demonstrated the potential to use LS301 to evaluate colonoscopic resection margins and guide intraoperative decisions.

Although LS301 binds to integrins at tumor margins, the identities of these integrins remain unknown. The study of integrins that play important roles at the interface between tumor and normal tissue may identify new targets for imaging tumor biology, such as local invasion and metastasis. Cancer cell metastasis is a convoluted process thought to involve a transition of epithelial to mesenchymal cell morphology allowing cell motility and dissemination from the original site. Metastasis is therefore believed to be caused by a decreased function in cell–cell adhesion. The loss of adhesion and spread of cancer cells suggest that the culprits for progression lie in the microenvironment of the tumor. Therefore, the border between cancerous and normal tissue is an attractive site for molecular imaging of cancer cell adhesion and motility.

In the process of colorectal tumorigenesis, major proteins involved in the regulation of cell adhesion include the adenomatous polyposis coli (APC) protein, E-cadherin,  $\beta$ -catenin, and  $\alpha$ -actinin 4. These proteins play important roles at the leading edges of epithelial and endothelial tissues, specifically at adherens junctions between cells. E-cadherin is a transmembrane cell adhesion molecule that forms a complex with  $\beta$ -catenin and actin filaments at its short cytoplasmic tail.<sup>15</sup> Cellular levels of  $\beta$ -catenin are controlled by a degradation complex containing the APC protein.<sup>16</sup> In up to 80% of colorectal abnormalities, from early adenomas to invasive carcinomas, the APC tumor suppressor gene is inactivated. The resulting loss or disablement of the APC protein leads to dysregulated expression of  $\beta$ -catenin and its translocation to the nucleus, where it activates the oncogenic Wnt signaling pathway.<sup>17</sup> In addition, E-cadherin regulates the interaction of  $\beta$ -catenin with

$\alpha$ -actinin 4.<sup>18</sup> In the absence of E-cadherin,  $\alpha$ -actinin 4 binds to  $\beta$ -catenin, which results in the formation of exogenous protrusions, such as bleb-like structures, filopodia, and lamellipodia, where motility is fostered.<sup>18</sup> Changes in the complex interactions between these factors can result in loss of adhesion, tumor cell motility, local invasion, and metastasis of cancer cells.

In 2007, Amos-Landgraf et al developed the heterozygous *Apc*<sup>Pirc/+</sup> (Pirc) rat model with a stop codon at position 1137 of the APC gene.<sup>19</sup> The Pirc rat forms tumors preferentially in the large intestine, similar to the human clinical presentation. Incidence of extensive polyposis in the colon was 100% by 4 months of age. A percentage of these adenomas also progressed from early adenomas to adenocarcinomas. Thus, the Pirc rat was established as a new animal model of APC mutation in spontaneous CRC. Mutations in the APC gene lead to the transformation of normal epithelium into dysplastic aberrant crypt foci.<sup>20</sup> The resulting loss of function of APC disrupts processes that routinely prevent progression from normal to cancerous tissue.

We have evaluated Achilefu's peptide in the APC mutant Pirc rat model of CRC by colonoscopy and colonoscopic tumor removal. We have also evaluated its intratumoral distribution and specificity of targeting. We determined the ability of LS301 to detect tumor cells sufficiently on the leading edge of CRC polyps and flat and sessile lesions in Pirc rats. Using NIR fluorescence microscopy of these tumors, further assessments of LS301 uptake at the margins of lesions were performed.

## Materials and Methods

### Study Design

A derivative of LS301, Cy7.5-LS301 (also denoted LS301 in this article), in which the cypate dye of the parent peptide was replaced with the structural analogue Cy7.5, was synthesized using standard solid-phase peptide synthesis methods and Cy7.5 NHS ester (Lumiprobe, Hallandale Beach, Florida). Cy7.5 has approximately the same excitation (788 nm) and emission (808 nm) properties as cypate, as well as the same depth of penetration (2.91 mm) in colon tissue.<sup>21</sup> Colorectal tumor-bearing Pirc rats were subjected to colonoscopy by conventional white light, narrow band, and NIR imaging using Cy7.5-LS301, for detection of early-stage flat lesions and for evaluation of surgical resection of established tumors.

### Animals

Pirc rats were generated by crossing male, F344/Ntac-*Apc*<sup>+/-am1137</sup> Pirc rats<sup>19</sup> with wild-type females from the colony (generations, n = 31). They were pair-housed on ventilated racks (Thoren, Hazleton, Pennsylvania) in microisolator cages. Cages were furnished with paper chip bedding, and the rats were fed irradiated 5058 PicoLab Mouse Diet 20 (LabDiet, St Louis, Missouri). Rats had ad libitum access to water purified by sulfuric acid (pH 2.5–2.8) treatment followed by

autoclaving. All procedures were performed according to the guidelines regulated by the Guide for the Use and Care of Laboratory Animals, the Public Health Service Policy on Humane Care and Use of Laboratory Animals, and the Guidelines for the Welfare of Animals in Experimental Neoplasia and were approved by the University of Missouri Institutional Animal Care and Use Committee.

### Genotyping

Pirc rats that develop spontaneous colonic tumors are heterozygous for the *APC* tumor suppressor gene mutation. Breeding of Pirc male rats with wild-type females produces both heterozygous and wild-type animals in each litter. (The homozygous mutation is embryonic lethal; thus, Pirc rats are not crossed to each other.) Genotyping of animals was performed to ensure that no nontumor-bearing wild-type rats would inadvertently be used for experiments. All rats selected for these studies were confirmed to carry the Pirc mutation.

Pups were ear-punched prior to weaning at 12 days of age using sterile technique. DNA was extracted using the “HotSHOT” genomic DNA preparation method previously outlined.<sup>22</sup> Briefly, ear punches were collected into an alkaline lysis reagent (25 mM NaOH and 0.2 mM EDTA at a pH of 12). The ear clips were heated at 90°C on a heat block for 1 hour, followed by addition of the neutralization buffer (40 mM Tris-HCl) and vortexing for 5 seconds. DNA, thus obtained, was used for a high resolution melt analysis as described previously.<sup>23</sup>

### White Light, Narrow Band, and Targeted NIR Colonoscopy

Colonoscopies were performed longitudinally as described previously<sup>23,24</sup> on rats as early as 45 days of age, with follow-up procedures on a monthly schedule. Briefly, 3% isoflurane was used to anesthetize rats. They were then placed with the ventral side down on a sterile field, covering a heating pad to ensure body temperature maintenance during the procedure. An enema was performed using 1× phosphate-buffered saline (PBS; Fisher Scientific Co LLC, Pittsburg, California), to remove fecal and colonic contents, as well as to lubricate the colon prior to inserting a semirigid endoscope rectally. Video and still images were recorded from the proximal to the distal colon with both white light and NBI, using the EVIS EXERA III, CLV-190 system (Olympus America Inc, Lombard, Illinois). The NBI was used for the potential identification of neoplastic and nonneoplastic lesions, along with observing mucosal and vascular structure during the colonoscopies.<sup>25</sup>

A miniaturized system equipped with an NIR confocal laser was constructed for acquisition of fluorescence images during colonoscopy. This system (Figure 1) consisted of a semirigid endoscope connected to a 20 mW, 785 nm excitation source, with a spatial resolution of 2.4 × 3.4 mm at 3 m. However, the laser was positioned less than 1 m from the working end of the scope for the present studies, minimizing divergence of the beam. The system was also equipped with 800 nm short-

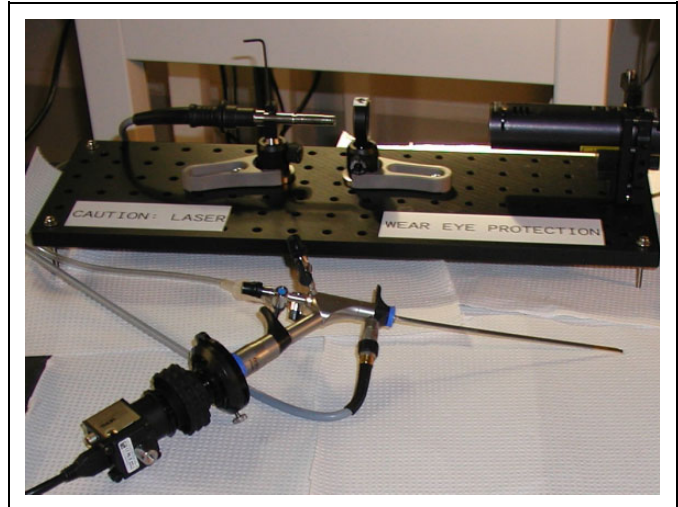


**Figure 1.** Near-infrared laser system for fluorescence-guided colonoscopy. Foreground: Semirigid colonoscope with charged coupled device (CCD) camera and 800 nm long-pass filter. Background (left to right): Light guide, 800 nm short-pass filter, 785 nm laser source.

pass and long-pass filters for wavelength-specific signal acquisition, a light guide, a 350 to 1100 nm charged coupled device (CCD) camera, and a real-time video monitor. Still frame and video images were captured as the scope was withdrawn.

Cy7.5-LS301 was synthesized by CPC Scientific, Inc (Sunnyvale, California). The NIR peptide-guided colonoscopy using the peptide was executed on rats aged 45 days to 7 months ( $n = 4$ , 2 males and 2 females). After being given the PBS enema, rats were given a cold topical colonic application of a 60  $\mu$ M Cy7.5-LS301 sol-gel formulation<sup>14</sup> (10% Pluronic F-127 in PBS, pH 7.4), and the rectum was held closed to allow permeation of the sol-gel. After 10 minutes, the colon was washed 3 to 5 times with warm PBS. The rats were killed at the end of the study, and the lesions were excised for further study. Gross necropsy of the colon and small intestine was performed for identification of tumors.

### Near-Infrared Fluorescence Microscopy

Formalin-fixed, paraffin-embedded tissues were sectioned at 4  $\mu$ m and dried at room temperature for 30 minutes. Slides were heated at 60°C for 30 minutes, deparaffinized with 100% xylene, and rehydrated in a gradient of ethanol. Pretreatment was performed using sodium citrate buffer, pH 6 (Dako Antigen Retrieval; DAKO S1699, Carpinteria, California) at 95°C in a steamer for 20 minutes. The sections were allowed to cool 20 minutes, rinsed 3 times with distilled water, and allowed to stand in PBS, pH 7.4, twice for 5 minutes. The sections were blocked with 1% bovine serum albumin for 20 minutes before incubation with Cy7.5-LS301 (100  $\mu$ L of a 10  $\mu$ M solution) overnight at 4°C in a humidity chamber. The following day the slides were warmed to room temperature, rinsed with multiple PBS washes, and dried for 10 minutes before coverslipping with 4',6-diamidino-2-phenylindole (DAPI) (Vectashield, H-

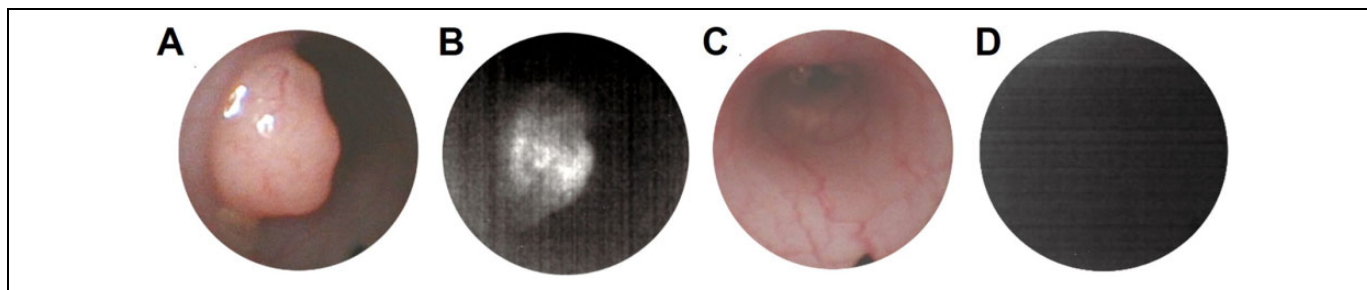


**Figure 2.** Visible and near-infrared (NIR) colonoscopy of a Pirc rat. A, Early adenoma (2 mm) detected by conventional white light colonoscopy. B, Cy7.5-LS301 NIR image of the same tumor. C, Normal tissue. D, Near-infrared image of the same normal tissue.

1200; Vector Laboratories, Burlingame, California). Coverslips were then sealed with fingernail polish. Rat kidney was used as a positive control, and in the negative control, the peptide was replaced with diluent.

Slides were imaged using wide-field Zeiss (Oberkochen, Germany) Axiovert 200 M microscopes, utilizing the bright-field setting of a Leica DFC290 color camera or the Cy7, Cy5, and DSRed fluorescent filters with the Hamamatsu ORCA-ER CCD camera, respectively, for high-resolution imaging. The objective EC Plan-Neofluar 10 $\times$ /0.3 magnification was used to acquire composite images of the tissue slices. This system operates with the MetaMorph software v.7.8.12.

### Immunofluorescence

$\beta$ -catenin rat/human monoclonal mouse IgG2b clone #196621 (MAB1329-SP; 1:40 dilution) was purchased from R&D Systems (Minneapolis, Minnesota). E-cadherin antibody (G-10) mouse monoclonal IgG1 $\kappa$  (sc8426; 1:100 dilution) was purchased from Santa Cruz (Dallas, Texas). ACTNIN4 Ab59468 rabbit polyclonal (1:200 dilution) was purchased from AbCam (Cambridge, Massachusetts).

Formalin-fixed, paraffin-embedded tissues were sectioned at 4  $\mu$ m and dried at room temperature for 30 minutes. Slides were heated at 60 $^{\circ}$ C for 30 minutes and deparaffinized and rehydrated in a gradient of ethanol. Pretreatment was performed using sodium citrate buffer, pH 6.0, for  $\beta$ -catenin and ACTNIN4 (Dako Antigen Retrieval; DAKO S1699) or EDTA for E-cadherin (DAKO S2368). Solutions were heated at 95 $^{\circ}$ C in a steamer for 20 minutes. The sections were permeabilized with 1% goat serum in PBS with 0.4% Triton X-100 for 10 minutes, followed by blocking with 5% goat serum for 30 minutes. Sections were incubated with the primary antibodies for 60 minutes at room temperature, and protein was detected with the secondary antibodies Alexa Fluor 594 antirabbit IgG, Alexa Fluor 488 antimouse IgG1, or Alexa Fluor 647 antimouse IgG (H&L; Life Technologies, Carlsbad, California) for 45 minutes at room temperature. After washing the sections with PBS, Cy7.5-LS301 (10  $\mu$ M) was applied, and the slides were incubated overnight at 4 $^{\circ}$ C in a humidity chamber. The following day the slides were warmed to room temperature, rinsed with multiple PBS washes, and dried for 10 minutes before coverslipping with DAPI (Vectashield, H-1200; Vector

Laboratories). Coverslips were sealed with fingernail polish. Rat kidney was used for positive control tissues, and negative control consisted of no peptide or no primary antibody followed by the secondary antibody.

### Polypectomy

Rats age 7 months ( $n = 4$ , 2 male, 2 female) underwent polypectomy using an electrocautery snare connected to the working channel of the endoscope. Follow-up was performed by white light, narrow band, and NIR fluorescence colonoscopy at 3 days, 3 weeks, and 5 weeks postsurgery. Then animals were euthanized, and the colon and small intestine were examined macroscopically at necropsy for the presence of gastrointestinal lesions.

## Results

### Evaluation of Tumor Specificity

As proof of principle, a Pirc rat with an established 2-mm early adenoma underwent conventional white light (Figure 2A) and targeted NIR colonoscopy using LS301 (Figure 2B), respectively. The tumor was clearly detected by NIR imaging, plainly showing the borders between the sessile lesion and surrounding normal tissue. In normal colon (Figure 2C), no signal was observed (Figure 2D), indicating a lack of autofluorescence in healthy tissue.

### Detection of Flat Lesions

At 45 days of age, Pirc rats have not generally developed macroscopic adenomas. Figure 3A-C shows white light, narrow band, and Cy7.5-LS301-targeted NIR colonoscopy of three 45-day-old rats. Images from the 3 modes of detection were lined up by pinpointing the depth of the scope in regions of interest, at 4.0, 6.5, and 5.5 mm proximal to the rectal sphincter for rats A, B, and C, respectively. As seen in Figure 3, white light (left) and narrow band (middle) colonoscopy were negative in these regions. However, targeted NIR imaging (right) clearly showed lesions in the 3 rats not detected by the other 2 modalities. At gross necropsy, hematoxylin and eosin staining (far right) confirmed that the lesions detected by NIR colonoscopy were flat tumors, as opposed to some other

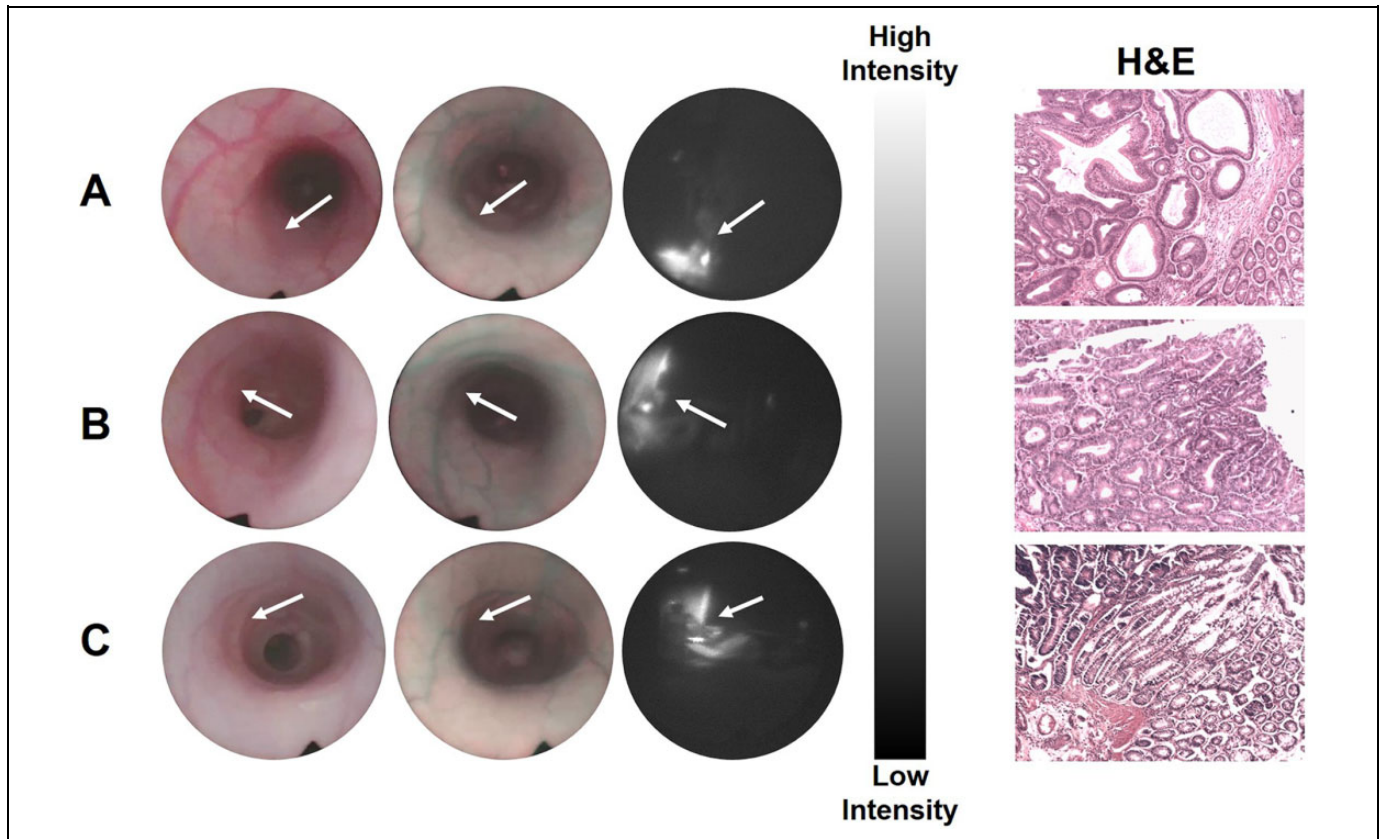


**Figure 3.** White light (left), narrow band (middle), and LS301-targeted near-infrared (NIR; right) colonoscopy of three 45-day-old Pirc rats (A, B, C). The arrows point to the location of the lesions. Hematoxylin and eosin staining of the tumors is shown on the far right.

condition such as an inflammatory process. A fourth rat was negative for the development of polyps.

### Near-Infrared Fluorescence Microscopy

Corresponding adjacent slices of the tumors were evaluated by NIR fluorescence microscopy (Figure 4). DAPI staining (left) was used to establish the cellular anatomy of each tumor. Near-infrared imaging (center) showed the intratumoral uptake of Cy7.5-LS301. A merged image (right) showed that the peptide predominantly targets the border between tumor and normal tissue in the rat model.

### Immunofluorescence

Immunofluorescence studies were performed to evaluate colocalization of Cy7.5-LS301 with components of the E-cadherin/ $\beta$ -catenin/ $\alpha$ -actinin 4 adhesion complex (Figure 5). Merged images of the peptide and the respective proteins showed that LS301 colocalized with E-cadherin and  $\beta$ -catenin. However, the peptide did not show any colocalization with  $\alpha$ -actinin 4.

### Fluorescence-Guided Polypectomy

Colonoscopic polypectomies were performed on the same rats at 7 months of age. Figure 6 shows the removal of a polyp

(Figure 6A) from one rat, followed by the development of fibrosis within 3 days (Figure 6B). The bright-field image at 3 weeks postsurgery showed a suspicious, raised focal area at the top of the field of view (Figure 6C), but the NIR image showed no accumulation of LS301 (Figure 6D). Continued lack of NIR fluorescence at the resection site 5 weeks postsurgery (Figure 6E) demonstrated negative margins indicative of successful surgery.

### Discussion

In this study, we showed that image-guided colonoscopy using NIR targeting with LS301 is effective for the identification and removal of colonic polyps in a rat model of adenoma development. This technique addresses a critical area of need in CRC management, with significant potential for improvement in patients' lives by both earlier detection and avoidance of potentially morbid surgery.

In the initial studies performed by Achilefu and coworkers, LS301 was conjugated to the dye cypate. We used the cypate derivative Cy7.5 to prepare the peptide conjugate used in the present studies. As opposed to the more commonly used Cy5.5, we chose Cy7.5 because its excitation (788 vs 684 nm for Cy5.5) and emission (808 vs 710 nm for Cy5.5) occur at longer wavelengths and produce a greater depth of tissue penetration. Thus, Cy7.5 may allow tumors more deeply seated in the colon

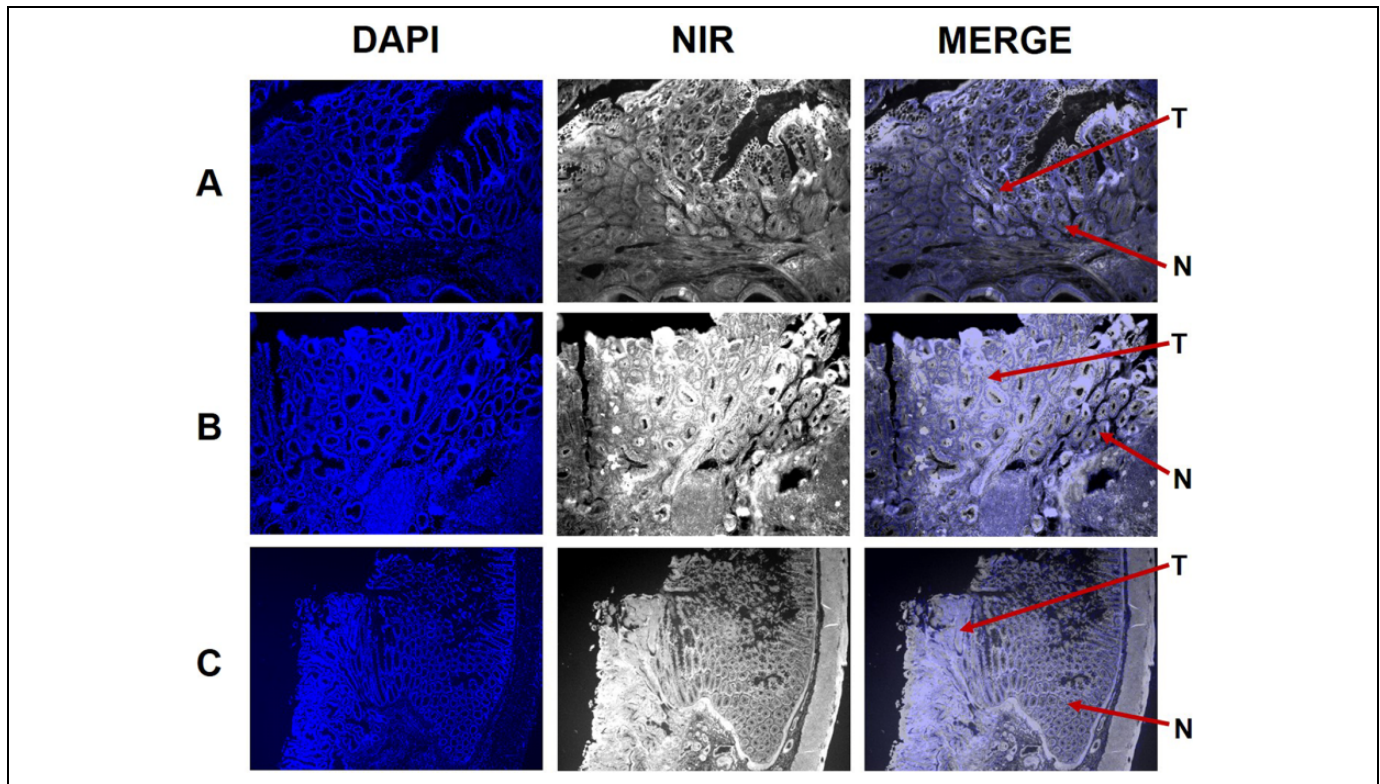


**Figure 4.** DAPI staining (left), near-infrared fluorescence microscopy using Cy7.5-LS301 (center), and merged images (right) of the rat flat tumors shown in Figure 3. The peptide localizes to tumor tissue (T) to a greater degree than to adjacent normal tissue (N).

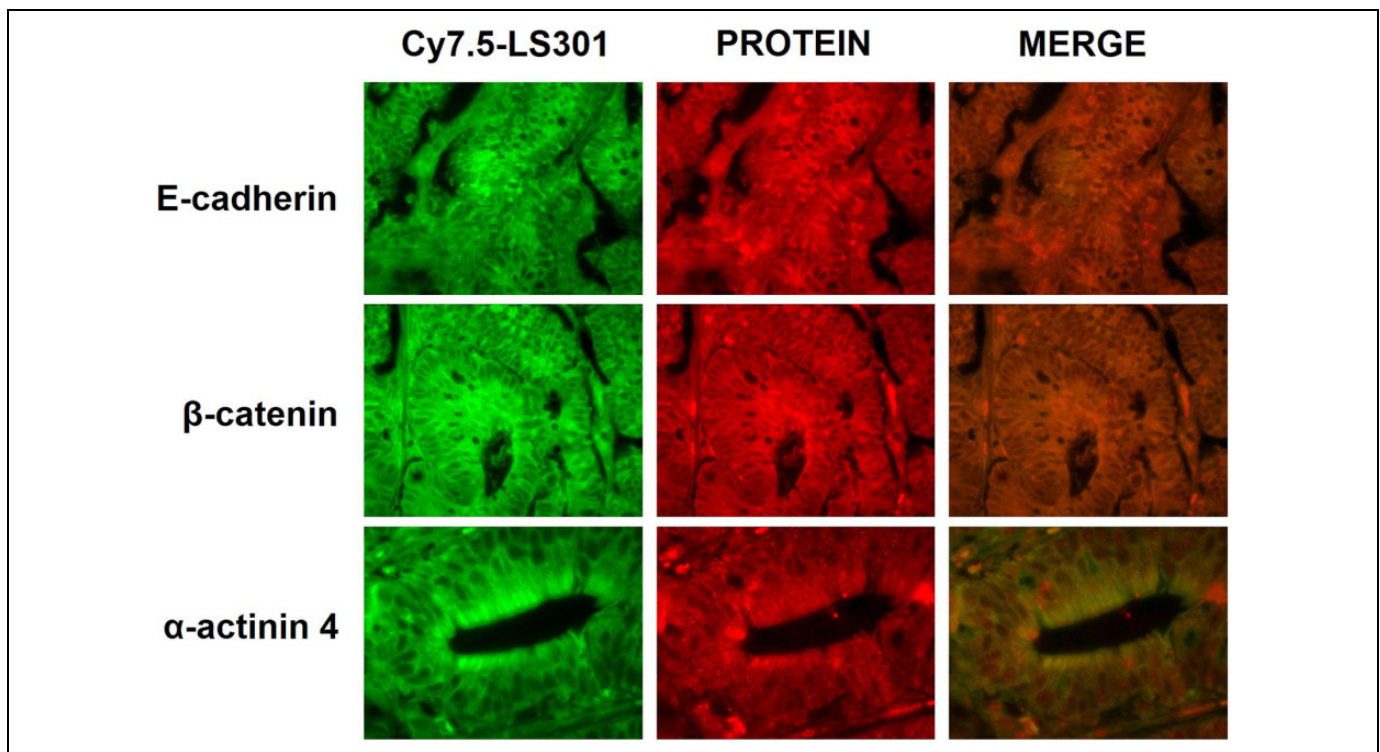


**Figure 5.** Immunofluorescence images of Cy7.5-LS301 (left), adhesion complex proteins (center), and merged (right) of the Pirca rat adenoma shown in Figure 3C.

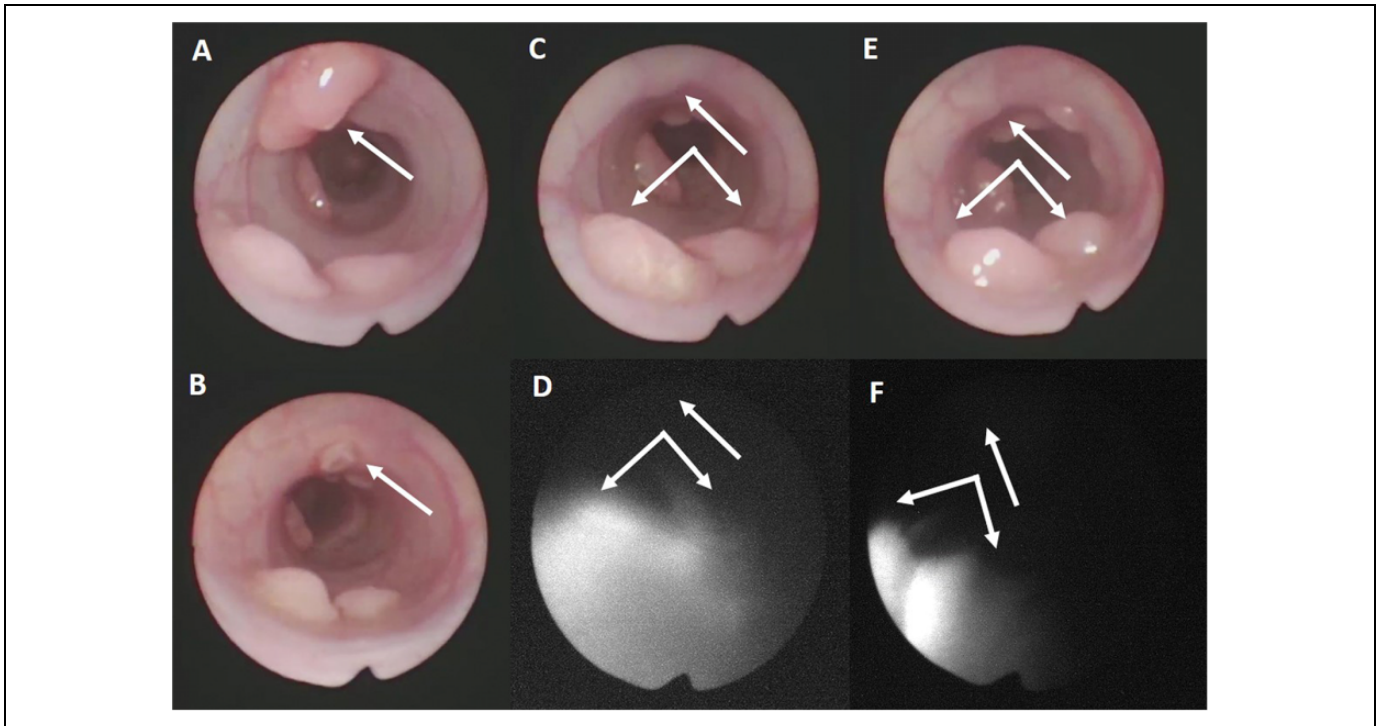


**Figure 6.** Polypectomy of a 7-month-old Pirc rat. A, Polyp before removal. B, Resection site 3 days postsurgery. C, Resection site 3 weeks postsurgery. D, Near-infrared image of the resection site 3 weeks postsurgery. E, Resection site 5 weeks postsurgery. F, Near-infrared image of the resection site 5 weeks postsurgery. The 2 tumors at the bottom of the images were deliberately left to provide an anatomic reference.

to be detected. In addition, the rigid linker in the fluorophore of Cy7.5 gives it a greater fluorescence quantum yield, which should improve the sensitivity of tumor imaging.

As discussed above, endoscopic colon screening decreases the rate of death from colon cancer.<sup>26</sup> However, colonoscopy still experiences significant limitations. Despite improved technology, the adenoma miss rate is >20%. Lesions that are typically missed and are difficult to identify include flat or small tumors.<sup>3</sup> Tumors that are flat are more common in right-sided lesions and are more likely to harbor advanced features at a smaller size, making them both high risk for being missed and for expedited progression.<sup>27</sup> Clinical relevance is the demonstration of less impact of colonoscopy on the death rate for right-sided CRC<sup>26</sup> and higher rates of “missed” cancers in the right colon.<sup>28</sup> It is clear from these data that improved lesion detection is needed to prevent presentation with advanced disease. Newer advanced imaging technologies aimed at improving detection have shown limited utility. Some of these limitations are related to the technology itself, such as light penetrance. One additional very important limiting factor is the nonspecific nature of the modalities. Despite all the improvements in technology, currently accepted advanced imaging techniques still rely heavily on the expertise of the endoscopist to interpret the image. The novel technology we have evaluated here offers the potential of improved detection not only by greater light penetrance but also by providing specific targeting and decreasing the inherent limitations of human interpretation by targeting cells directly.

Assessment of margin status is an important factor to ensure adequacy of lesion removal endoscopically. Positive margin status is predictive of both local and metastatic recurrence.<sup>6</sup> Due to the critical nature of margin negative resection, the current recommendation for patients with cancer containing polyps and a positive margin is to undergo segmental colectomy.<sup>29</sup> Although it is standard to remove all visually abnormal tissue during endoscopic resection, it is impossible to grasp true margin negativity determined by pathologic examination. The data we present using LS301 suggest that the peptide is differentially directed at lesion margins. Utilizing this targeted system, we have the potential to ensure more accurately the adequacy of resection and avoid the potential morbidity of colonic resection in these patients.

It has been reported that LS301 binds integrin receptors at the border between tumor and normal tissue. Our immunofluorescence studies suggest that there may be an interaction of LS301 with E-cadherin and  $\beta$ -catenin in the *APC* mutant rat model, but not with the  $\alpha$ -actinin 4 scaffold upon which the complex is built. Thus, if LS301 binds specifically to this complex in the Pirc rat, it more likely associates with E-cadherin and  $\beta$ -catenin than with  $\alpha$ -actinin 4. More definitive studies will have to be performed to determine whether LS301 binds components of this adhesion complex specifically. In addition, it is important to consider that the functions of other adhesion molecules may also play a role in the localization of LS301 to tumor margins.

A limitation of the present studies is that we employed topical application of Cy7.5-LS301 in the rat model. We chose this route of administration to be consistent with the technique Charanya et al used for NIR colonoscopy of tumor-bearing mice.<sup>14</sup> However, topical application of an NIR peptide is not clinically practical, due to the large quantity of the imaging agent that would be needed. We have now established an optimal intravenous injected dose in Pirc rats and will use this method of administration for future studies.

We have not yet tested our ability to detect recurrent disease in the rat model. We plan to evaluate the ability of the peptide to do so in longer term longitudinal studies. In the future, we will evaluate Cy7.5-LS301 for early detection and endoscopic resection of CRC lesions in *APC* knockout pigs carrying floxed p53 and LSL G12V-activated *K-RAS* mutations, a large mammalian model of inducible invasive adenocarcinoma.

### Acknowledgments

The authors are grateful to Dr Diane McConnell for invaluable assistance with the histopathology and fluorescence microscopy. The authors also thank Dr Samuel Achilefu of Washington University in St. Louis for helpful discussions, as well as the Department of Veterans Affairs for the use of facilities and resources at the Harry S. Truman Memorial Veterans' Hospital in Columbia, Missouri.

### Declaration of Conflicting Interests

The author(s) declared no potential conflicts of interest with respect to the research, authorship, and/or publication of this article.

### Funding

The author(s) disclosed receipt of the following financial support for the research, authorship, and/or publication of this article: This work was funded by a grant from the Ellis Fischel Cancer Center, by a Faculty Research Award from the University of Missouri College of Veterinary Medicine and by a grant from the University of Missouri Research Board.

### References

1. Siegel RL, Miller KD, Fedewa SA, et al. Colorectal cancer statistics, 2017. *CA Cancer J Clin.* 2017;67(3):177–193.
2. van Rijn JC, Reitsma JB, Stoker J, Bossuyt PM, van Deventer SJ, Dekker E. Polyp miss rate determined by tandem colonoscopy: a systematic review. *Am J Gastroenterol.* 2006;101(2):343–350.
3. Heresbach D, Barrioz T, Lapalus MG, et al. Miss rate for colorectal neoplastic polyps: a prospective multicenter study of back-to-back video colonoscopies. *Endoscopy.* 2008;40(4):284–290.
4. Compton CC, Fielding LP, Burgart LJ, et al. Prognostic factors in colorectal cancer. College of American Pathologists Consensus Statement 1999. *Arch Pathol Lab Med.* 2000;124(7):979–994.
5. Lieberman DA, Weiss DG, Bond JH, Ahnen DJ, Garewal H, Chejfec G. Use of colonoscopy to screen asymptomatic adults for colorectal cancer. Veterans Affairs Cooperative Study Group 380. *N Engl J Med.* 2000;343(3):162–168.
6. Butte JM, Tang P, Gonen M, et al. Rate of residual disease after complete endoscopic resection of malignant colon polyp. *Dis Colon Rectum.* 2012;55(2):122–127.
7. Pasha SF, Leighton JA, Das A, et al. Comparison of the yield and miss rate of narrow band imaging and white light endoscopy in patients undergoing screening or surveillance colonoscopy: a meta-analysis. *Am J Gastroenterol.* 2012;107(3):363–370.
8. Stallmach A, Schmidt C, Watson A, Kiesslich R. An unmet medical need: advances in endoscopic imaging of colorectal neoplasia. *J Biophotonics.* 2011;4(7-8):482–489.
9. Matsuda T, Saito Y, Fu KI, et al. Does autofluorescence imaging videoendoscopy system improve the colonoscopic polyp detection rate?—a pilot study. *Am J Gastroenterol.* 2008;103(8):1926–1932.
10. Takeuchi Y, Inoue T, Hanaoka N, Chatani R, Uedo N. Surveillance colonoscopy using a transparent hood and image-enhanced endoscopy. *Dig Endosc.* 2010;22(suppl 1):S47–S53.
11. Liu Y, Akers WJ, Bauer AQ, et al. Intraoperative detection of liver tumors aided by a fluorescence goggle system and multimodal imaging. *Analyst.* 2013;138(8):2254–2257.
12. Liu Y, Njuguna R, Matthews T, et al. Near-infrared fluorescence goggle system with complementary metal-oxide-semiconductor imaging sensor and see-through display. *J Biomed Opt.* 2013;18(10):101303.
13. Liu Y, Bauer AQ, Akers WJ, et al. Hands-free, wireless goggles for near-infrared fluorescence and real-time image-guided surgery. *Surgery.* 2011;149(5):689–698.
14. Charanya T, York T, Bloch S, et al. Trimodal color-fluorescence-polarization endoscopy aided by a tumor selective molecular probe accurately detects flat lesions in colitis-associated cancer. *J Biomed Opt.* 2014;19(2):126002.
15. Liu S, Barry EL, Baron JA, Rutherford RE, Seabrook ME, Bostick RM. Effects of supplemental calcium and vitamin D on the APC/ $\beta$ -catenin pathway in the normal colorectal mucosa of colorectal adenoma patients. *Mol Carcinog.* 2017;56(2):412–424.
16. MacDonald BT, Tamai K, He X. Wnt/ $\beta$ -catenin signaling: components, mechanisms, and diseases. *Dev Cell.* 2009;17(1):9–26.
17. Peifer M, Polakis P. Wnt signaling in oncogenesis and embryogenesis—a look outside the nucleus. *Science.* 2000;287(5458):1606–1609.
18. Hayashida Y, Honda K, Idogawa M, et al. E-Cadherin regulates the association between  $\beta$ -catenin and actinin-4. *Cancer Res.* 2005;65(19):8836–8845.
19. Amos-Landgraf JM, Kwong LN, Kendzierski CM, et al. A target-selected *Apc*-mutant rat kindred enhances the modeling of familial human colon cancer. *Proc Natl Acad Sci U S A* 2007;104(10):4036–4041.
20. Kinzler KW, Vogelstein B. Lessons from hereditary colorectal cancer. *Cell.* 1996;87(2):159–170.
21. Stolik S, Delgado JA, Pérez A, Anasagasti L. Measurement of the penetration depths of red and near infrared light in human “ex vivo” tissues. *J Photochem Photobiol B.* 2000;57(2-3):90–93.
22. Truett GE, Heeger P, Mynatt RL, Truett AA, Walker JA, Warman ML. Preparation of PCR-quality mouse genomic DNA with hot sodium hydroxide and tris (HotSHOT). *Biotechniques.* 2000;29(1):52–54.
23. Ericsson AC, Akter S, Hanson MM, et al. Differential susceptibility to colorectal cancer due to naturally occurring gut microbiota. *Oncotarget.* 2015;6(32):33689–33704.

24. Irving AA, Young LB, Pleiman JK, et al. A simple, quantitative method using alginate gel to determine rat colonic tumor volume in vivo. *Comp Med*. 2014;64(2):128–134.
25. Sakamoto T, Matsuda T, Aoki T, Nakajima T, Saito Y. Time saving with narrow-band imaging for distinguishing between neoplastic and non-neoplastic small colorectal lesions. *J Gastroenterol Hepatol*. 2012;27(2):351–355.
26. Baxter NN, Warren JL, Barrett MJ, Stukel TA, Doria-Rose VP. Association between colonoscopy and colorectal cancer mortality in a US cohort according to site of cancer and colonoscopist specialty. *J Clin Oncol*. 2012;30(21):2664–2669.
27. Rondagh EJ, Bouwens MW, Riedl RG, et al. Endoscopic appearance of proximal colorectal neoplasms and potential implications for colonoscopy in cancer prevention. *Gastrointest Endosc*. 2012;75(6):1218–1225.
28. Bressler B, Paszat LF, Chen Z, Rothwell DM, Vinden C, Rabeneck L. Rates of new or missed colorectal cancers after colonoscopy and their risk factors: a population-based analysis. *Gastroenterology*. 2007;132(1):96–102.
29. Aarons CB, Shanmugan S, Bleier JI. Management of malignant colon polyps: current status and controversies. *World J Gastroenterol*. 2014;20(43):16178–16183.